Gastrin Enhances the Angiogenic Potential of Endothelial Cells via Modulation of Heparin-Binding Epidermal-Like Growth Factor

Philip A. Clarke, Jacqueline H. Dickson, Joseph C. Harris, Anna Grabowska, and Susan A. Watson

Academic Unit of Cancer Studies, University of Nottingham, Queen's Medical Centre, University Hospital, Nottingham, United Kingdom

Abstract

This study examined whether gastrin modulates endothelial cell activity via heparin-binding epidermal growth factor–like growth factor (HB-EGF) expression. Human umbilical vascular endothelial cells (HUVEC) were assessed for tubule formation in the presence of amidated gastrin-17 (G17) and glycine-extended gastrin-17 (GlyG17) peptides. HB-EGF gene and protein expressions were measured by quantitative reverse transcription-PCR, immunocytochemistry, and Western blotting, and HB-EGF shedding by ELISA. Matrix metalloproteinases MMP-2, MMP-3, and MMP-9 were assessed by Western blotting. Chick chorioallantoic membrane studies measured the *in vivo* angiogenic potential of gastrin and microvessel density (MVD) was assessed in large intestinal premalignant lesions of hypergastrinaemic APC^{Min} mice. MVD was also examined in human colorectal tumor and resection margin normals and correlated with serum-amidated gastrin levels (via RIA) and HB-EGF protein expression (via immunohistochemistry). HUVEC cells showed increased tubule and node formation in response to G17 (186%, $P < 0.0005$) and GlyG17 (194%, $P < 0.0005$). This was blockaded by the cholecystokinin-2 receptor (CCK-2R) antagonists JB95008 and JMV1155 and by antiserum to gastrin and HB-EGF. Gastrin peptides increased HB-EGF gene expression/protein secretion in HUVEC and microvessel-derived endothelial cells and the levels of MMP-2, MMP-3, and MMP-9. G17 promoted angiogenesis in a chorioallantoic membrane assay, and MVD was significantly elevated in premalignant large intestinal tissue from hypergastrinaemic APC^{Min} mice. In terms of the clinical situation, MVD in the normal mucosa surrounding colorectal adenocarcinomas correlated with patient serum gastrin levels and HB-EGF expression. Gastrin peptides, acting through the CCK-2R, enhance endothelial cell activity in models of angiogenesis. This may be mediated through enhanced expression and shedding of HB-EGF, possibly resulting from increased activity of matrix metalloproteinases. This proangiogenic effect translates to the *in vivo* and human situations and may add to the tumorigenic properties attributable to gastrin peptides in malignancy. (Cancer Res 2006; 66(7): 3504-12)

Introduction

Gastrin peptides have multiple carcinogenic activities in gastrointestinal adenocarcinomas through both autocrine/paracrine and endocrine mechanisms (1). Mature amidated gastrin peptides act through the G-protein–coupled cholecystokinin-2/gastrin receptor (CCK-2R), which mediates the normal endocrine activities of gastrin, such as acid secretion. The classic CCK-2R, together with a number of splice variants, have been shown to play a role in malignancy (2–4).

Gastrin gene transcription is normally tightly regulated but may be elevated in the cancer situation, as it is a transcriptional target of β-catenin (5, 6). Post-translational processing of preprogastrin is also disordered in malignant epithelial cells, resulting in constitutive release of poorly processed gastrin forms, such as progastrin, and glycine-extended gastrin species (7). Nonamidated gastrin peptides, such as glycine-extended gastrin-17 (GlyG17), possess biological activity that includes pro-proliferative effects on epithelial cells and enhancement of carcinogen-induced tumorigenicity in the colon (8, 9).

Gastrin peptides increase the transcription of a number of key target genes associated with tumorigenesis, including cyclooxygenase-2 (*COX-2*), plasminogen activator inhibitor-2 (*PIA-2*), the regenerating protein (*Reg*; refs. 10–12), and matrix metalloproteinase (MMP) enzymes (13–15). Importantly, much emphasis has been placed on the ability of gastrin to both up-regulate ligands of the epidermal growth factor (EGF) receptor, in particular amphiregulin and heparin-binding EGF-like growth factor (HB-EGF; refs. 16–18). The effect of gastrin on both the shedding of EGF receptor growth factors and related downstream signaling pathways has received particular attention. In terms of a proangiogenic role for gastrin, a recent study showed such an *in vivo* in a glioma model involving E-selectin activation (19).

Our study has explored the role of gastrin peptides on the angiogenic potential of human endothelial cell lines through mediation of HB-EGF expression and shedding. Two gastrin peptides were compared; gastrin-17 (G17), the form involved in endocrine pathways and GlyG17, a form secreted by tumor cells themselves and ascribed a role as an autocrine factor (20). It was confirmed that both G17 and GlyG17 increased tubule formation of human endothelial cells grown on an extracellular matrix and enhanced HB-EGF expression and shedding. MMP-2, MMP-3, and MMP-9 expression also increased, with these factors potentially playing a role in regulating shedding of the HB-EGF. *In vivo* models confirmed the proangiogenic effects of G17, and these translated to the clinical situation based on the observation that there is increased vessel density and elevated HB-EGF protein expression in the normal mucosa surrounding colorectal adenocarcinomas in patients with elevated serum-amidated gastrin levels.

Note: P.A. Clarke and J.H. Dickson are joint first authors.

Requests for reprints: Susan A. Watson, Academic Unit of Cancer Studies, D Floor, West Block, Queen's Medical Centre, University Hospital, Nottingham, NG7 2UH, United Kingdom. Phone: 44-115-9709248; Fax: 44-115-9709902; E-mail: sue.watson@nottingham.ac.uk.

doi:10.1158/0008-5472.CAN-05-0280

Materials and Methods

Human endothelial monocultures. Human umbilical vein endothelial cells (HUVEC), uterine microvascular endothelial cells (UtMVEC), and dermal microvascular endothelial cells (HMVEC-D; Cambrex, Walkersville, MD) were cultured in EGM-2 with 2% fetal bovine serum (HUVEC) and EGM-MV microvascular specific medium with the recommended Single Quot supplementation including 5% fetal bovine serum, bovine brain extract, hydrocortisone, and human EGF (both Cambrex). Subconfluent cells were harvested with 0.25% trypsin and 0.03% EDTA solution (both Sigma, Poole, Dorset, United Kingdom).

Human angiogenesis model. This comprised a human angiogenesis system (TCS CellWorks, Buckingham, United Kingdom) consisting of irradiated human fibroblast cell monolayers seeded with HUVEC. Medium was replenished on days 1, 4, and 7 supplemented with G17, GlyG17 (both Aphton Corp., Woodland, CA), or a scrambled gastrin peptide control AL55 (WGDGF-NH_2, Biopolymer Synthesis and Analysis Unit, University of Nottingham, Nottingham, United Kingdom) at concentrations between 10 μmol/L and 10 pmol/L. Dose response studies confirmed 10 nmol/L as the optimal G17 and GlyG17 concentration, and it was this concentration that was used in all subsequent studies. Suramin (20 mmol/L) and vascular endothelial growth factor ($VEGF_{165}$; 20 μg/mL) were used as negative and positive controls, respectively (TCS CellWorks). The compound treatments remained constant throughout the duration of the experiment from initiation on day 1 through to termination on day 9 with refeeding on days 1, 4, and 7. On day 9, the cells were fixed in 70% ethanol, and tubule formation was visualized with an endothelial tubule staining kit (TCS CellWorks). Briefly, tubules were labeled with murine monoclonal anti-human CD31 (platelet/endothelial cell adhesion molecule 1) cell surface antigen antibody for 60 minutes and immunolocalized using a goat anti-mouse alkaline phosphatase secondary for a further 60 minutes. 5′-Bromo-4-chloro-3-indolyl phosphate chromagen with nitro blue tetrazolium enhancer was incubated for 30 minutes giving an insoluble purple precipitate.

This model follows HUVEC development from proliferation through to differentiation/maturation and has a branching tubule phenotype, with each branch point classified as a node. Node formation was measured by assessing 10 to 20 fields in each duplicate-coded well, with two observers in a blinded system, interobserver variation being <10%. Mean node development across treatments was compared by a one-way ANOVA statistical test.

Inhibition of angiogenic differentiation using gastrin-neutralizing antibodies and specific antagonists. A rabbit anti-G17DT antiserum, raised against the NH_2- terminal nine amino acids of G17 coupled to diphtheria toxoid [G17-DT (Insegia), Aphton], which neutralizes both the COOH-amidated and glycine-extended forms of G17 with affinities of 0.15 and 0.47 nmol/L, respectively (21), was introduced at 10 μg/mL, and its effects were compared against 10 μg/mL of purified normal rabbit serum control (Aphton). Reversal of G17 and GlyG17 effects was assessed using the specific CCK-2R antagonists YM022 and JB95008 (Gastrazole; ref. 22), at concentrations of 10^{-6} mol/L.

Reverse transcription and PCR amplification. RNA extraction was done as previously described using RNABee (Biogenesis, Poole, United Kingdom), and cDNA was synthesized as described previously (2). PCR reactions were carried out using the qPCR Core kit for SYBR Green I (Eurogentec, Romsey, United Kingdom) in a GeneAmp 5700 Sequence Detector Real-time PCR machine (Applied Biosystems, Warrington, United Kingdom) following the program: 50°C for 2 minutes, 95°C for 10 minutes then 40 cycles of 95°C for 15 seconds, and 60°C for 1 minute (Applied Biosystems). The sequences of the primers used were as follows: HB-EGF sense, CTCTTTCTGGCTGCAGTTCTC; HB-EGF antisense, AGCTGGTCC-GTGGATACAGT; hypoxanthine phosphoribosyltransferase (HPRT) sense, GACCAGTCAACAGGGGACAT; HPRT antisense, CGACCTTGACCATC-TTTGGA.

Results are presented as relative gene expression compared with that for the house-keeping gene *HPRT* and a reference treatment by the $2^{-\Delta\Delta Ct}$ method (23), using the following equation, where Ct represents the number of cycles required to reach an arbitrary fluorescence threshold during the linear phase of amplification

$$\text{Relative gene expression} = 2^{\frac{[Ct_{(HB-EGF)} - Ct_{(HPRT)}]_{\text{test condition}}}{[Ct_{(HB-EGF)} - Ct_{(HPRT)}]_{\text{reference condition}}}}$$

Statistical assessment was done using a one-way ANOVA test.

Western analysis. Cell lysates from HUVEC cell cultures were analyzed under denaturing and reducing conditions on 8% to 16% gradient Tris/glycine gels (Invitrogen, Paisley, United Kingdom). Resolved proteins were transferred to polyvinylidene difluoride membranes (Invitrogen), blocked with 5% nonfat dry milk, then washed thrice in TBST [20 mmol/L Tris, 0.5 mol/L NaCl (pH 7.5), and 0.05% Tween 20]. Membranes were incubated overnight at 4°C with goat anti-MMP-2, anti-MMP-3, and anti-MMP-9 (R&D Systems, Abingdon, United Kingdom) at 1 mg/mL concentration or goat IgG (as a negative control), an anti-goat secondary antibody (DakoCytomation, Ely, United Kingdom) was added, and immune complexes were visualized using enhanced chemiluminescence Plus (Amersham Biosciences, Little Chalfont, United Kingdom). Gel analysis was done on a Syngene Chemigenius 2 BioImaging System, using GeneTools Software.

Immunofluorescent staining of cytospins. Approximately 1×10^4 formalin-fixed cells (0.4%) were spun onto Polysine slides (VWR, Lutterworth, United Kingdom), washed twice in PBS (pH 7.2) for 5 minutes each and incubated for 5 minutes in PBS with 0.5% Triton X-100. Cells were incubated for 30 minutes at room temperature in PBS with 3% bovine serum albumin (BSA) and 1% glycine, then PBS containing 10% rabbit serum. Goat anti HB-EGF (C-18; Santa Cruz Biotechnology, Santa Cruz, CA) was added overnight at 4°C followed by incubation with the secondary antibody, Alexa Fluor 594 goat anti-rabbit in 10% normal goat serum. Slides were washed and coverslipped using the SlowFade Antifade Light kit with 4′,6-diamidino-2-phenylindole (Molecular Probes, Eugene, OR) and analyzed using QWin image analysis software (Leica Microsystems, Milton Keynes, United Kingdom).

HB-EGF ELISA. Culture medium or control medium (not incubated with cells) was collected, clarified by centrifugation, and concentrated to 150 μL using Centriplus-10 concentrators with a molecular weight cutoff of 10,000 (Amicon, Beverly, MA). Serial dilutions of human recombinant HB-EGF (Sigma), at 0.03 to 128 ng/mL, or concentrated conditioned media were added at 50 μL/well in 96-well Maxisorp Nunc-immuno plates (Fisher Scientific, Loughborough, United Kingdom) and incubated overnight at 4°C. The plate was washed with PBS-Tween and blocked with 5% BSA in PBS-Tween for 2 hours at 37°C. Goat anti-human HB-EGF (R&D Systems) was added at 1 μg/mL, and the plate was incubated overnight at 4°C. Binding was detected using biotinylated rabbit anti-goat immunoglobulin (1:10,000 dilution, DakoCytomation), streptavidin-HRP (1:5,000 dilution, DakoCytomation), and 3,3′,5,5′-tetramethylbenzidine (Sigma). The reaction was stopped with 0.5 mol/L H_2SO_4, and the absorbance was read at 450 nm. The standard curve was linear between 0.03 and 32 ng/mL HB-EGF, and cell conditioned media absorbance values were converted to ng/mL values based on the linear regression transformation of the standard curve. Statistical assessment was done using a one-way ANOVA test.

Chick chorioallantoic membrane studies. The chorioallantoic membrane model used in this study was modified from that used by Melkonian et al. (24), briefly, fertilized white broiler chicken eggs were incubated at 37°C until stage 19 of development (day 3.5). Eggs were opened from the air sack end, and 3 mL of egg white was removed to allow the embryo to drop away from the shell, providing space for compound treatment. The positive control angiopoietin-1 (1 μg/mL), G17 (10 nmol/L), or the vehicle control solution were dotted onto sterile nitrocellulose filter discs (10 μL per disc) presoaked in a 3 mg/mL solution of cortisone acetate (in absolute ethanol, to reduce inflammation) and then air-dried before use. The discs were placed, one per egg on the left vitalline artery (LVA), and the eggs were sealed with tape and returned to 37°C for a further 24 hours.

After incubation the tape was removed and observations were made using the untreated right vittaline artery (RVA) in each egg for comparison.

Human primary tumor sample collection and storage. Samples were collected from 31 freshly resected human colorectal tumors from Nottingham University Hospital, Department of Surgery. Ethical permission was granted from the Queen's Medical Centre Ethical Review Committee, Nottingham, United Kingdom. Samples of tumor and nonmalignant mucosa (from the resection margin and >10 cm from the cancer) were formalin fixed, processed, and embedded in paraffin wax. Fasting sera were obtained from patients before surgical excision and were assayed for levels of

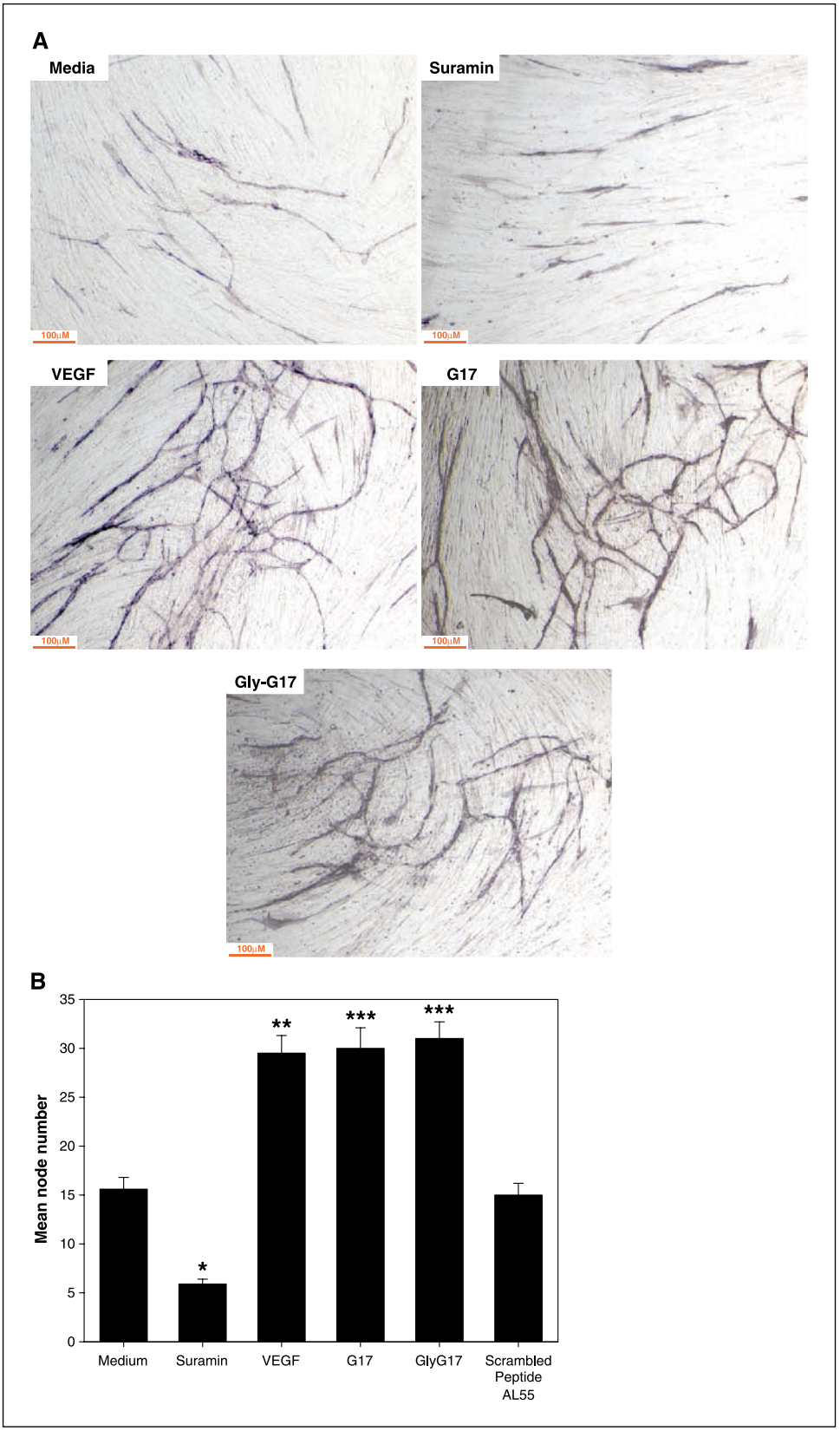

Figure 1. Effect of G17 and GlyG17 on HUVEC node formation in *in vitro* culture. *A,* microscopic images. HUVEC tubule and node formation over a 9-day culture period are shown for medium alone and in the presence of suramin (20 nmol/L), VEGF (20 ng/mL), G17 (10 nmol/L), or GlyG17 (10 nmol/L). Red bar, 200 μm. *B,* effect of G17 and GlyG17 on mean node number. *Columns,* mean node formation for two separate experiments with $n = 2$ to 3 replicates per condition within each experiment; *bars,* SE. Suramin significantly inhibited node formation from 16.0 (medium control) to 6.0 (*, $P < 0.0005$). VEGF significantly increased node number to 29.5 (**, $P < 0.0005$). G17 and GlyG17 produced growth effects equal to VEGF with a mean node number of 30 and 31, respectively (***, $P < 0.0005$). The scrambled peptide AL55 had no significant effect on node formation and was significantly different from effects of G17 and GlyG17 (both $P = 0.0005$).

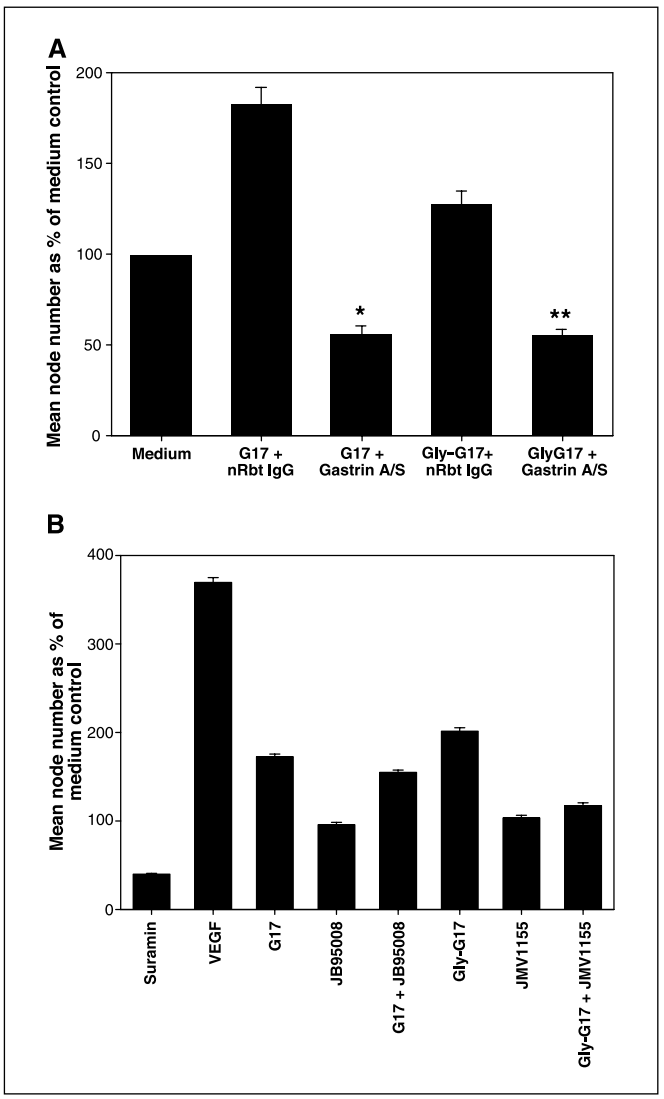

Figure 2. Inhibition of gastrin-induced effects on HUVEC node formation. *A,* neutralization with rabbit anti-gastrin antiserum (*A/S*). Gastrin antiserum significantly reduced node formation in the presence of G17 from 183% to 56% of the medium control (*, $P < 0.0001$) and of GlyG17 from 128% to 55% of the medium control (**, $P < 0.0001$; $n = 2$ separate experiments, two to three replicates per condition). *B,* CCK-2R blockade of the actions of G17 and GlyG17. JB95008 reversed the G17-induced effect on HUVEC node formation from 171% to 82% (*, $P < 0.0001$). JMV reversed the GlyG17-induced effect on HUVEC node formation from 201% to 117% (**, $P = 0.04$) of the medium control.

amidated G17 by RIA (25) at the Physiology Laboratory, University of Liverpool, United Kingdom under the supervision of Dr. A. Varro. All data obtained from tissue were transformed to an ordinal (ranked format) for statistical assessment using a Spearman's rho correlation test.

Immunohistochemistry on human and mouse tissue sections. Paraffin-embedded sections of colorectal tissue were attached to polysine glass slides (VWR). CD31 immunohistochemistry was carried out via indirect streptavidin/biotin labeling of murine anti-human CD31 (clone JC70A, DakoCytomation). Endogenous peroxidase was removed by a 0.6% hydrogen peroxidase block. Nonspecific protein/protein interactions were reduced by preincubation with 20% rabbit serum. Endogenous biotin and associated binding proteins were reduced by pretreatment with a streptavidin/biotin blocking system (Vector Laboratories, Burlingame, CA). Visualization was via diaminobenzidine tetrahydrochloride liquid system (DAB, DakoCytomation).

CD34 immunohistochemistry was carried out on paraffin-embedded APC^{Min} mouse large intestinal tissue as described above with the following amendments; antigen unmasking was via citric acid microwave antigen retrieval (10 mmol/L citric acid, pH 6). Endogenous peroxidase was removed by 3% hydrogen peroxide blockade. Primary antibodies, rat anti-mouse CD34, and concentration-matched rat IgG2a control (BD Biosciences PharMingen, Oxford, United Kingdom) were labeled with polyclonal anti-rat biotinylated secondary (BD Biosciences PharMingen).

Microvessel density was measured according to Vermeulen et al. (26). Briefly, hotspot areas of CD31-labeled or CD34-labeled events were counted over $n = 8$ fields of view at ×10 (CD31) and ×40 (CD34) objective magnification under bright-field microscopy.

Progastrin immunohistochemistry was carried out using rabbit polyclonal antiserum raised against the COOH terminus as previously described (24).

COOH-terminal HB-EGF immunohistochemistry was carried out by horseradish peroxidase (HRP)–conjugated secondary labeling of goat polyclonal anti-HB-EGF(C-18)/sc1413 (Santa Cruz Biotechnology), Endogenous peroxidase was removed with 3% hydrogen peroxidase block, and nonspecific protein/protein interactions were reduced by preincubation with 20% rabbit serum. Microwave antigen retrieval was carried out using prewarmed 10 mmol/L citric acid (pH 6) heated at half power for 10 minutes with 20-minute cooling time. Rabbit anti goat-HRP secondary (DakoCytomation) was used according to manufacturer's instruction. Visualization was via liquid DAB system (DakoCytomation).

Results

The influence of gastrin peptides on HUVEC differentiation. The effect of gastrin peptides on tubule/node formation in HUVECs cultured on a fibroblast feeder layer was studied. In this model, HUVECs appeared initially as distinct "islands" within the fibroblast monolayer. As the experiment progressed, they underwent proliferation and migration to form thread-like tubule structures, which joined to form a network of anastomosing tubules. Thus, the growth characteristics of this model provide data on both proliferation (early stages) and differentiation (later stages). Tubule branch points or nodes were counted as an indication of maturity of the tubule network.

G17 and GlyG17 were initially assessed in terms of HUVEC node formation at concentrations ranging from 10 μmol/L to 10 pmol/L. G17 and GlyG17 significantly stimulated growth, 353% control ($P = 0.002$) and 303% ($P = 0.011$), respectively, compared with 563% control for VEGF (2 ng/mL). However, 10 μmol/L and 10 pmol/L G17 and GlyG17 had no significant effect on node formation (data not shown). HUVEC node formation and mean node number in a range of growth conditions, including G17 and GlyG17, at optimal concentrations of 10 nmol/L, are shown in Fig. 1*A* and *B*, respectively. In the presence of the inhibitor suramin, mean node number was significantly reduced compared with the medium control that included all constituents of HUVEC growth medium without peptide supplementation (16.0 down to 6.0 mean nodes, 37% of control; $P < 0.0005$). The positive control, VEGF, significantly increased node number from the medium control (29.5 from 16.0 mean nodes, 184%; $P < 0.0005$) as did G17 (30.0 from 16.0, 187%; $P < 0.0005$) and GlyG17 (31.0 from 16.0, 193%; $P < 0.0005$). The scrambled gastrin peptide AL55 had no significant effect on node number. Furthermore, G17 and GlyG17 induced significant increased node formation compared with AL55 (both $P = 0.0005$).

Neutralization of the effect of gastrin peptides with an anti-gastrin antiserum and CCK-2 receptor antagonists. To further investigate whether the differentiation-inducing effect of gastrin was reversible and mediated through the CCK-2R, the experiment was repeated with the addition of either gastrin antiserum or

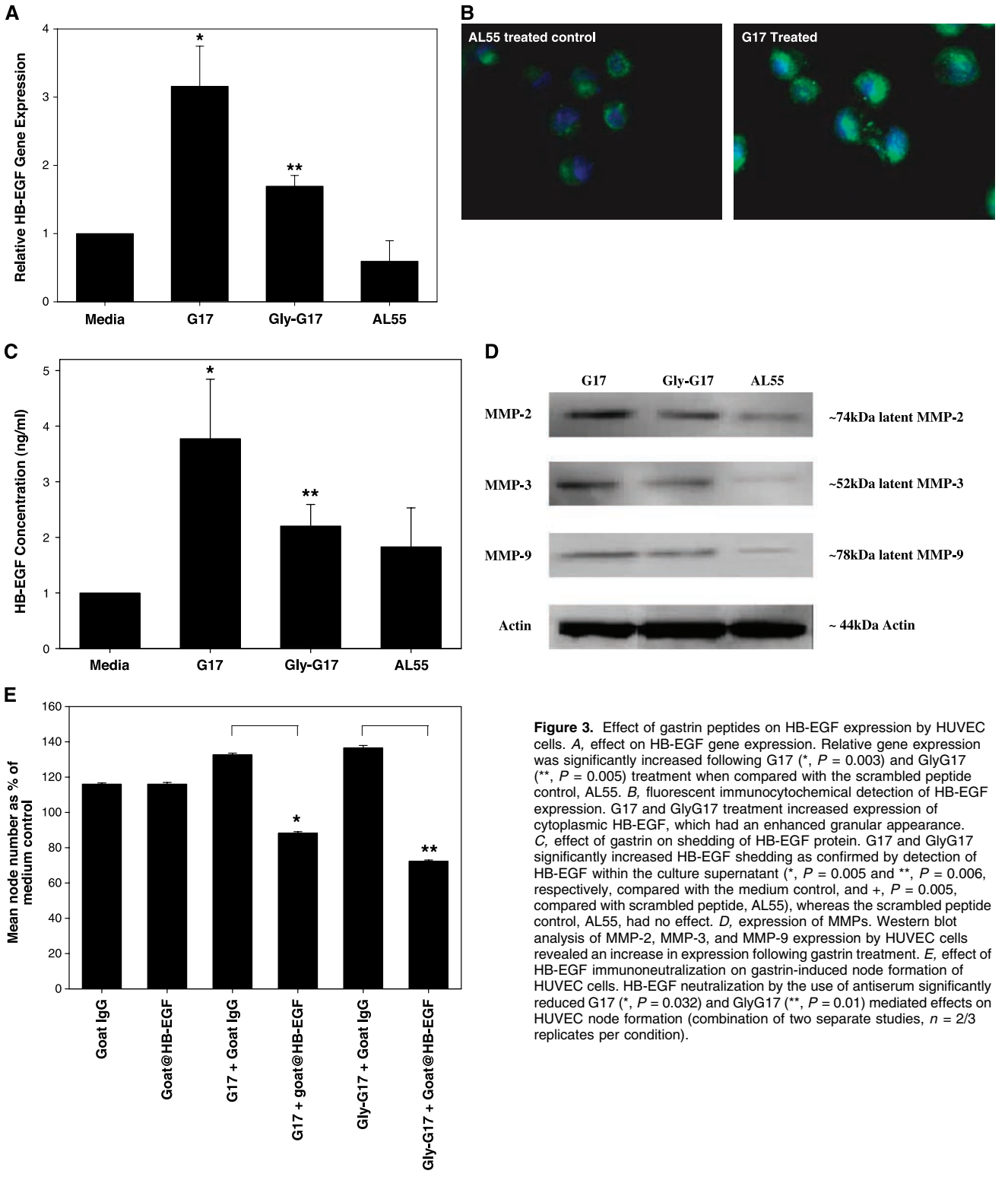

Figure 3. Effect of gastrin peptides on HB-EGF expression by HUVEC cells. *A,* effect on HB-EGF gene expression. Relative gene expression was significantly increased following G17 (*, $P = 0.003$) and GlyG17 (**, $P = 0.005$) treatment when compared with the scrambled peptide control, AL55. *B,* fluorescent immunocytochemical detection of HB-EGF expression. G17 and GlyG17 treatment increased expression of cytoplasmic HB-EGF, which had an enhanced granular appearance. *C,* effect of gastrin on shedding of HB-EGF protein. G17 and GlyG17 significantly increased HB-EGF shedding as confirmed by detection of HB-EGF within the culture supernatant (*, $P = 0.005$ and **, $P = 0.006$, respectively, compared with the medium control, and +, $P = 0.005$, compared with scrambled peptide, AL55), whereas the scrambled peptide control, AL55, had no effect. *D,* expression of MMPs. Western blot analysis of MMP-2, MMP-3, and MMP-9 expression by HUVEC cells revealed an increase in expression following gastrin treatment. *E,* effect of HB-EGF immunoneutralization on gastrin-induced node formation of HUVEC cells. HB-EGF neutralization by the use of antiserum significantly reduced G17 (*, $P = 0.032$) and GlyG17 (**, $P = 0.01$) mediated effects on HUVEC node formation (combination of two separate studies, $n = 2/3$ replicates per condition).

CCK-2R antagonists. Gastrin antiserum (10 μg/mL) neutralized the differentiating effects of exogenous G17 from 183% to 56% ($P < 0.0001$) and exogenous GlyG17 from 128% of the control medium to 55% ($P < 0.0001$; Fig. 2*A*).

Two CCK-2R antagonists were used to blockade the effects of the gastrin peptides: JB95008 (a competitor of amidated G17) and JMV1155 (a competitor of GlyG17). The effect of G17 was reversed from 171% to 82% ($P < 0.0001$) with JB95008, and the effect of

GlyG17 was reversed from 201% to 117% ($P = 0.04$) of the medium control with JMV1155 (Fig. 2*B*).

Effect of G17 and GlyG17 on HB-EGF gene expression and HB-EGF secretion by HUVEC cells. One of the potential mechanisms through which gastrin peptides may act upon vascular density/node formation of HUVEC cells is via up-regulation of HB-EGF. The effect of G17 and GlyG17 on HB-EGF gene and protein expression was compared with that of the scrambled peptide AL55 (Fig. 3*A*). G17 induced a 5.6-fold increase in HB-EGF gene expression compared with the scrambled peptide control ($P = 0.003$) and GlyG17 a 2.8-fold increase ($P = 0.005$). The effect with G17 was significantly greater than that achieved with GlyG17 ($P = 0.014$).

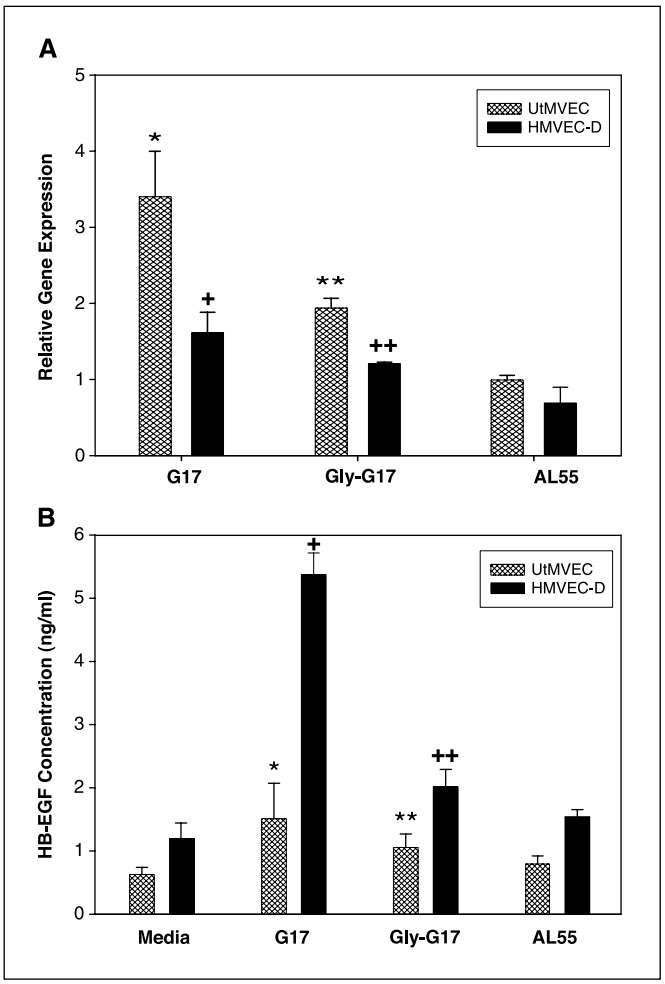

Figure 4. Effect of gastrin peptides on HB-EGF expression by the microvascular endothelial cells UtMVEC and HMVEC-D. *A,* effect on HB-EGF gene expression. Both G17 and GlyG17 significantly increased HB-EGF gene expression of UtMVEC (*, $P = 0.003$ and **, $P = 0.011$, respectively), whereas G17, but not GlyG17, increased gene expression of HMVEC-D (+, $P < 0.05$ and ++, $P = 0.072$, respectively; combined results for three separate experiments for UtMVEC and 2 for HMVEC-D with 3 replicates per condition) when compared with medium control. Both G17 and GlyG17 retained significance from AL55 ($P = 0.003$ and 0.005, respectively). *B,* effect on HB-EGF protein shedding. G17 and GlyG17 significantly increased HB-EGF secretion by UtMVEC (*, $P = 0.05$ and **, $P = 0.041$, respectively), whereas G17 but not GlyG17 increased shedding by HMVEC-D (+, $P = 0.05$ and ++, $P = 0.085$, respectively; combined results for three separate experiments for UtMVEC and two for HMVEC-D with three replicates per condition) when compared with medium control. Both G17 and GlyG17 retained significance from AL55 ($P = 0.005$ and 0.006, respectively).

HB-EGF expression was also increased at the protein level following treatment with G17 and GlyG17 (Fig. 3*B*). Under basal conditions, there was discrete cytoplasmic expression, whereas following G17 treatment staining appeared punctate/granular. A similar pattern of staining was seen in cells treated with GlyG17 (data not shown).

Treatment with G17 and GlyG17 had a significant effect on HB-EGF shedding into the cell supernatant during cell growth (Fig. 3*C*). G17 induced a 2.7-fold increase in shedding ($P = 0.005$) compared with a 1.75-fold increase ($P = 0.006$) for GlyG17, whereas there was no significant effect with the scrambled peptide (Fig. 3*C*) compared with cells treated with medium alone. G17 had a significantly enhanced effect compared with the scrambled peptide AL55 ($P = 0.005$), whereas GlyG17 did not significantly enhance shedding.

Role of MMP-2, MMP-3, and MMP-9 in gastrin-induced HB-EGF shedding. MMP-2, MMP-3, and MMP-9, which are known to be implicated in HB-EGF shedding (27, 28), were evaluated in HUVEC cell lysates following gastrin treatment. Both G17 and GlyG17 increased the expression level of all three MMPs when compared with cells treated with the scrambled peptide control (Fig. 3*D*). Up-regulation of MMP-2 and MMP-3 was most marked following treatment with G17.

Role of HB-EGF on gastrin-mediated HUVEC differentiation. To delineate the role of HB-EGF in increased node formation following both G17 and GlyG17 treatment, a neutralizing antibody was included in the culture system. HB-EGF antiserum significantly inhibited both the G17-mediated response (66.5% of G17 + control IgG, $P = 0.032$, ANOVA) and the GlyG17-mediated response (53% of GlyG17 + control IgG, $P = 0.001$), whereas it had no significant effect on the basal node formation of HUVEC cells (111% of medium control; Fig. 3*E*).

Effect of G17/GlyG17 on HB-EGF gene expression and secretion in UtMVEC and HMVEC-D human microvascular endothelial cells. The effect of G17 and GlyG17 on HB-EGF expression in the human microvascular endothelial cell lines UtMVEC (uterine) and HMVEC-D (dermal) was investigated. G17 and GlyG17 significantly stimulated UtMVEC HB-EGF gene expression (G17: 3.4-fold increase, $P = 0.03$; GlyG17: 1.9-fold increase, $P = 0.011$) when compared with medium control and also when compared with AL55. G17 but not GlyG17 significantly increased gene expression in HMVEC-D cells (G17: 2.1-fold increase, $P = 0.05$; GlyG17: 1.5-fold increase, $P = 0.072$; Fig. 4*A*) when compared with medium control or AL55.

G17 showed a trend to significantly increase UtMVEC secretion of HB-EGF (2.3-fold increase compared with medium control, $P = 0.053$), whereas GlyG17 had a significant effect (1.7-fold increase, $P = 0.041$; Fig. 4*B*) when compared with medium control and also when compared with AL55. G17 significantly increased HMVEC-D shedding of HB-EGF (4.5-fold, $P = 0.005$), whereas GlyG17 had no significant effect when compared with medium control and also when compared with AL55.

Effect of G17 on angiogenesis in an embryonic chick model. Angiogenic effects in the vicinity of the LVA were compared with the untreated RVA in the same embryo.

The vehicle control produced no noticeable effect on the LVA at the site of treatment (Fig. 5*A*). The standard positive control angiopoietin-1 produced proangiogenic effects in two of three chick embryos, including increased branching of the LVA and anterior vittaline vein (embryo 1) and increased disjointed branching of the LVA (embryo 2) with the third embryos showing no effect over control. G17 also produced proangiogenic effects in

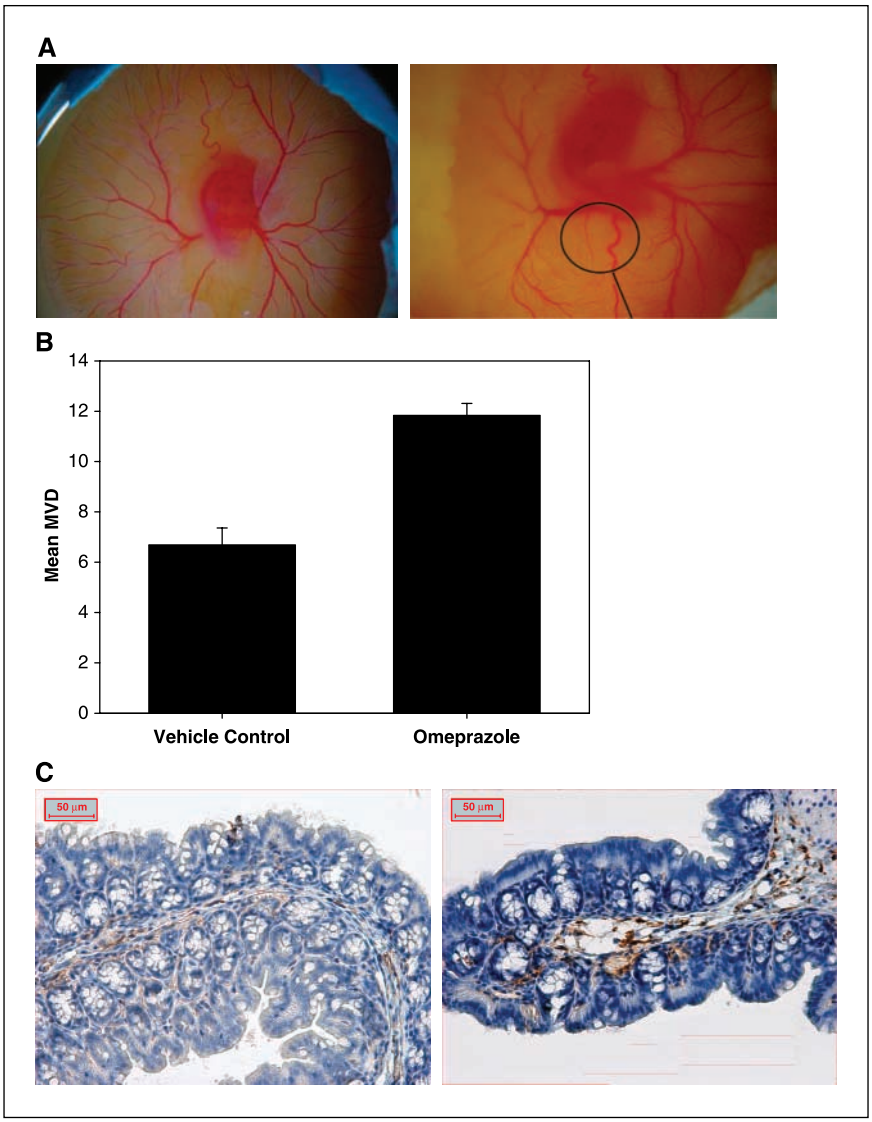

Figure 5. MVD in the large intestine. *A,* PBS vehicle control (*left*) and G17 treatment control (*right*) showing pronounced branching from the LVA (*circled*). *B,* omeprazole treatment of APC^{Min} mice significantly increased MVD in their large intestine compared with the vehicle control treated group ($P = 0.001$, one-way ANOVA; $n = 3$-4 mice/condition, $n = 8$ observations per section). *C,* CD34 labeling of APC^{Min} mice showing endothelial cells in omeprazole-treated (*right*) and vehicle control (*left*) large intestine.

two of three embryos, including generally increased branching throughout the chorioallantoic membrane, with pronounced branching stemming from the LVA at the site of compound treatment (embryo 1 and 3).

Effect of omeprazole-induced hypergastrinaemia on microvessel density of large intestine in the APC^{Min} mouse model. Histologic sections of APC^{Min} mouse large intestine treated with either vehicle control or the proton pump inhibitor omeprazole (n = 3-4 mice per condition) were assessed for microvessel density (MVD; n = 8 observations per section). Omeprazole treatment in the APC^{Min} mouse model is associated with hypergastrinaemia, and previous studies have shown that at the concentration used (75 mg/kg), serum gastrin levels can rise to 102 pmol/L (29). This elevation in gastrin was shown to correlate with a significant 2-fold increase in MVD as shown in Fig. 5*B* ($P = 0.001$, one-way ANOVA). Representative views of the angiogenic response in control and hypergastrinaemic mice are shown in Fig. 5*C*.

Relationship of serum-amidated gastrin levels to MVD in human colon tumors. To clarify the clinical significance of the previous findings, a series of 31 human colorectal primary tumor specimens and adjacent normal colonic mucosa were stained with antibodies directed against CD31 and HB-EGF to measure MVD. Staining intensity of both variables was related to fasting serum-amidated gastrin levels.

The MVD of resection margin normal colonic mucosa significantly correlated with fasting serum gastrin levels ($P = 0.003$, Pearson correlation = 0.524) and HB-EGF protein staining intensity ($P = 0.026$, correlation = 0.420), whereas tumor MVD showed a trend to correlating with fasting serum gastrin levels ($P = 0.07$) and significantly correlated with HB-EGF staining levels ($P = 0.015$, correlation = 0.438).

Discussion

The first study linking gastrin with increased gene expression of HB-EGF was in the rat gastric epithelial cell line RGM1, engineered to overexpress the CCK-2 receptor (17). Processing of cell-associated pro-HB-EGF to the secreted form was also enhanced by gastrin treatment. Gastrin-induced HB-EGF expression was confirmed as being via a PKC/extracellular signal-related kinase–dependent pathway (17). Furthermore, in hypergastrinaemic

transgenic mice shown to develop gastric cancer over a 20-month timeframe, HB-EGF was up-regulated within gastric mucosa at premalignant stages during cancer development (30).

In the current study, these findings have been extended to reveal that both amidated and glycine-extended G17 have a functional output in terms of angiogenesis, inducing node formation and branching in the genetically unmodified human umbilical vein endothelial cell line, HUVEC, to the same degree as VEGF. This is in agreement with the findings of Lefranc et al. in an *in vivo* glioma model (19). In this present study, the effects have been shown to be mediated via CCK-2 receptor isoforms, with CCK-2R antagonism reversing the angiogenic response induced by both peptides.

An *in vivo* pilot study using the chorioallantoic membrane system identified a potential proangiogenic role for G17. Increased angiogenesis was also showed in the APC^{Min} mouse model following proton pump inhibitor–induced hypergastrinaemia and in colonic tissue in hypergastrinaemic patients with colonic adenocarcinoma. These results suggest that gastrin-induced angiogenesis may play a role in cancer progression, particularly as CCK-2R have been shown to be expressed by a range of premalignant gastrointestinal lesions, including colonic polyps (31), intestinal metaplasia (32), and Barrett's esophagus (33).

G17 and GlyG17 both increased HB-EGF gene expression and pro-peptide processing to the secreted form in both HUVEC and microvessel-derived endothelial cell lines, with HB-EGF being implicated, at least in part, in the proangiogenic effects of gastrin as shown by the antiserum HB-EGF neutralization assays. Despite the presence of goat IgG reducing the overall sensitivity of HUVEC to G17 and GlyG17 (Fig. 3*E*), when comparing the two peptides, G17 seemed the more potent at stimulating HB-EGF gene and protein expression in all three endothelial cell lines tested. This may reflect different receptor subtypes that may potentially mediate the effects of GlyG17. HB-EGF is known to promote neovascularization *in vivo* (34), and this effect may therefore be enhanced in conditions of hypergastrinaemia, which occur in a number of clinical scenarios, such as *Helicobacter pylori* infection and following treatment with proton pump inhibitors (35).

There are multiple reports of MMP involvement in HB-EGF ectodomain shedding, and a number of members of this family have been identified as sheddases, including the stromelysins MMP-1 and MMP-3, gelatinases MMP-2 and MMP-9, and the matrilysin MMP-7 (27, 28, 36, 37). Gastrin-induced up-regulation of MMP-3, MMP-2, and MMP-9 in HUVEC cells was confirmed in the present study. Activation of all these MMPs by gastrin has previously been reported in other cell types (14, 15, 38).

The clinical relevance of these findings was shown by detection of increased MVD and HB-EGF expression in the normal mucosa at the margin of colorectal tumors in patients with elevated fasting serum-amidated gastrin levels, indicating this tissue represents a greater threat of becoming precancerous. A significant increase was not seen within the tumor itself (although MVD was shown to correlate with HB-EGF expression), potentially indicating that serum-associated gastrin may not affect tumor vasculation to the same degree as normal vasculation. This hypothesis could be explained by a number of factors, including degree of CCK-2R expression, vessel composition, differential cellular interactions, and expression of endogenous gastrin peptides. It also suggests that raised serum gastrin levels may increase angiogenic activity close to the tumor sites, possibly aiding in capillary sprouting into areas of hypoxia/necrosis (39–42).

This current study is the first to report an effect of gastrin on endothelial cells mediated by HB-EGF. Other gut-associated hormones have previously been shown to influence angiogenesis; for example, bombesin (a modulator of gastrin secretion) can stimulate proangiogenic factors, including VEGF and IL-8 via nuclear factor-κB in prostate cancer cells (43) and, in a separate study, has been shown to increase HB-EGF shedding and promote migration (44). A direct link, however, between angiogenic potential and enhanced expression by HB-EGF following bombesin treatment has not been reported. This present study hence helps to fill in a missing part of the angiogenesis story.

Taken together, the results presented here confirm the functional role in angiogenesis ascribed to gastrin (19) and show that this occurs via stimulation of HB-EGF expression/shedding, resulting in enhanced MMP expression. They add further evidence to the multifunctionality of gastrin ligands, suggesting a proangiogenic role in the vicinity of malignant cells and supporting their role in carcinogenesis. Based on these findings, therapeutic adjunct to chemotherapy/radiotherapy through CCK-2 receptor antagonists and gastrin vaccines, such as Insegia (G17DT), seems warranted.

Acknowledgments

Received 1/31/2005; revised 11/22/2005; accepted 12/14/2005.

The costs of publication of this article were defrayed in part by the payment of page charges. This article must therefore be hereby marked *advertisement* in accordance with 18 U.S.C. Section 1734 solely to indicate this fact.

We thank Dr. Siobhan Loughna for advice on the chorioallantoic membrane assay, the James Black Foundation for provision of the CCK-2 receptor antagonists, and Amanda Tobias for technical assistance.

References

1. Watson SA, Gilliam AD. G17DT: a new weapon in the therapeutic armoury for gastrointestinal malignancy. Expert Opin Biol Ther 2001;1:309–17.
2. McWilliams DF, Watson SA, Crosbee DM, Michaeli D, Seth R. Coexpression of gastrin and gastrin receptors (CCK-B and delta CCK-B) in gastrointestinal tumour cell lines. Gut 1998;42:795–8.
3. Hellmich MR, Rui XL, Hellmich HL, Fleming RY, Evers BM, Townsend CM. Human colorectal cancers express a constitutively active cholecystokinin-B/gastrin receptor that stimulates cell growth. J Biol Chem 2000;275:32122–8.
4. Miyake A. A truncated isoform of human CCK-B/gastrin receptor generated by alternative usage of a novel exon. Biochem Biophys Res Commun 1995;208:230–7.
5. Koh TJ, Bulitta CJ, Fleming JV, Dockray GJ, Varro A, Wang TC. Gastrin is a target of the beta-catenin/TCF-4 growth-signaling pathway in a model of intestinal polyposis. J Clin Invest 2000;106:533–9.
6. Pradeep A, Sharma C, Sathyanarayana P, et al. Gastrin-mediated activation of cyclin D1 transcription involves beta-catenin and CREB pathways in gastric cancer cells. Oncogene 2004;23:3689–99.
7. Ciccotosto GD, McLeish A, Hardy KJ, Shulkes A. Expression, processing, and secretion of gastrin in patients with colorectal carcinoma. Gastroenterology 1995;109:1142–53.
8. Singh P, Velasco M, Given R, Varro A, Wang TC. Progastrin expression predisposes mice to colon carcinomas and adenomas in response to a chemical carcinogen. Gastroenterology 2000;119:162–71.
9. Aly A, Shulkes A, Baldwin GS. Short term infusion of glycine-extended gastrin(17) stimulates both proliferation and formation of aberrant crypt foci in rat colonic mucosa. Int J Cancer 2001;94:307–13.
10. Slice LW, Hodikian R, Zhukova E. Gastrin and EGF synergistically induce cyclooxygenase-2 expression in Swiss 3T3 fibroblasts that express the CCK2 receptor. J Cell Physiol 2003;196:454–63.
11. Varro A, Hemers E, Archer D, et al. Identification of plasminogen activator inhibitor-2 as a gastrin-regulated gene: role of Rho GTPase and menin. Gastroenterology 2002;123:271–80.
12. Ashcroft FJ, Varro A, Dimaline R, Dockray GJ. Control of expression of the lectin-like protein Reg-1 by gastrin: role of the Rho family GTPase RhoA and a C-rich promoter element. Biochem J 2004;381:397–403.
13. Kermorgant S, Lehy T. Glycine-extended gastrin promotes the invasiveness of human colon cancer cells. Biochem Biophys Res Commun 2001;285:136–41.
14. Wroblewski LE, Pritchard DM, Carter S, Varro A.

Gastrin-stimulated gastric epithelial cell invasion: the role and mechanism of increased matrix metalloproteinase 9 expression. Biochem J 2002;365:873–9.
15. Baba M, Itoh K, Tatsuta M. Glycine-extended gastrin induces matrix metalloproteinase-1- and -3-mediated invasion of human colon cancer cells through type I collagen gel and Matrigel. Int J Cancer 2004;111:23–31.
16. Tsutsui S, Shinomura Y, Higashiyama S, et al. Induction of heparin binding epidermal growth factor-like growth factor and amphiregulin mRNAs by gastrin in the rat stomach. Biochem Biophys Res Commun 1997;235:520–3.
17. Miyazaki Y, Shinomura Y, Tsutsui S, et al. Gastrin induces heparin-binding epidermal growth factor-like growth factor in rat gastric epithelial cells transfected with gastrin receptor. Gastroenterology 1999;116:78–89.
18. Sinclair NF, Ai W, Raychowdhury R, et al. Gastrin regulates the heparin-binding epidermal-like growth factor promoter via a PKC/EGFR-dependent mechanism. Am J Physiol Gastrointest Liver Physiol 2004;286: G992–9.
19. Lefranc F, Chaboteaux C, Belot N, Brotchi J, Salmon I, Kiss R. Determination of RNA expression for cholecystokinin/gastrin receptors (CCKA, CCKB and CCKC) in human tumors of the central and peripheral nervous system. Int J Oncol 2003;22:213–9.
20. Negre F, Fagot-Revurat P, Bouisson M, Rehfeld JF, Vaysse N, Pradayrol L. Autocrine stimulation of AR4–2J rat pancreatic tumor cell growth by glycine-extended gastrin. Int J Cancer 1996;66:653–8.
21. Watson SA, Michaeli D, Grimes S, et al. Gastrimmune raises antibodies that neutralize amidated and glycine-extended gastrin-17 and inhibit the growth of colon cancer. Cancer Res 1996;56:880–5.
22. Chau I, Cunningham D, Russell RCG, et al. Gastrazole, a novel CCK-b/gastrin receptor antagonist in the treatment of advanced pancreatic cancer: results from two randomised controlled trials. Eur J Cancer 2003;1:S69.
23. Litvak DA, Hellmich MR, Iwase K, et al. JMV1155: a novel inhibitor of glycine-extended progastrin-mediated growth of a human colon cancer *in vivo*. Anticancer Res 1999;19:45–9.
24. Melkonian G, Le C, Zheng W, Talbot P, Martins-Green M. Normal patterns of angiogenesis and extracellular matrix deposition in chick chorioallantoic membranes are disrupted by mainstream and sidestream cigarette smoke. Toxicol Appl Pharmacol 2000;163:26–37.
25. Nemeth J, Taylor B, Pauwels S, Varro A, Dockray GJ. Identification of progastrin derived peptides in colorectal carcinoma extracts. Gut 1993;34:90–5.
26. Vermeulen PB, Gasparini G, Fox SB, et al. Quantification of angiogenesis in solid human tumours: an international consensus on the methodology and criteria of evaluation. Eur J Cancer 1996;32A:2474–84.
27. Suzuki M, Raab G, Moses MA, Fernandez CA, Klagsbrun M. Matrix metalloproteinase-3 releases active heparin-binding EGF-like growth factor by cleavage at a specific juxtamembrane site. J Biol Chem 1997;272: 31730–7.
28. Roelle S, Grosse R, Aigner A, Krell HW, Czubayko F, Gudermann T. Matrix metalloproteinases 2 and 9 mediate epidermal growth factor receptor transactivation by gonadotropin-releasing hormone. J Biol Chem 2003;278:47307–18.
29. Watson SA, Smith AM. Expression of gastrin in developing gastric adenocarcinoma. Br J Surg 2001;88: 1543–3.
30. Wang TC, Dangler CA, Chen D, et al. Synergistic interaction between hypergastrinemia and *Helicobacter* infection in a mouse model of gastric cancer. Gastroenterology 2000;118:36–47.
31. Smith AM, Watson SA. Gastrin and gastrin receptor activation: an early event in the adenoma-carcinoma sequence. Gut 2000;47:820–4.
32. Henwood M, Clarke PA, Smith AM, Watson SA. Expression of gastrin in developing gastric adenocarcinoma. Br J Surg 2001;88:564–8.
33. Harris JC, Clarke PA, Awan A, Jankowski J, Watson SA. An antiapoptotic role for gastrin and the gastrin/CCK-2 receptor in Barrett's esophagus. Cancer Res 2004;64:1915–9.
34. Abramovitch R, Neeman M, Reich R, et al. Intercellular communication between vascular smooth muscle and endothelial cells mediated by heparin-binding epidermal growth factor-like growth factor and vascular endothelial growth factor. FEBS Lett 1998;425:441–7.
35. Takhar A, Watson SA. Gastrin interactions with the adenoma-carcinoma sequence of the colon. In: Merchant JL, Buchan AMJ, Wang TC, editors. Gastrin in the new millennium. Vol. Chapter 28. Los Angeles (CA): CURE Foundation; 2004. p. 329–38.
36. Sawa M, Kiyoi T, Kurokawa K, et al. New type of metalloproteinase inhibitor: design and synthesis of new phosphonamide-based hydroxamic acids. J Med Chem 2002;45:919–29.
37. Yu WH, Woessner JF, Jr., McNeish JD, Stamenkovic I. CD44 anchors the assembly of matrilysin/MMP-7 with heparin-binding epidermal growth factor precursor and ErbB4 and regulates female reproductive organ remodeling. Genes Dev 2002;16:307–23.
38. Nagakawa O, Ogasawara M, Fujii H, et al. Effect of prostatic neuropeptides on invasion and migration of PC-3 prostate cancer cells. Cancer Lett 1998; 133:27–33.
39. Shweiki D, Neeman M, Itin A, Keshet E. Induction of vascular endothelial growth factor expression by hypoxia and by glucose deficiency in multicell spheroids: implications for tumor angiogenesis. Proc Natl Acad Sci U S A 1995;92:768–72.
40. Shweiki D, Itin A, Soffer D, Keshet E. Vascular endothelial growth factor induced by hypoxia may mediate hypoxia-initiated angiogenesis. Nature 1992; 359:843–5.
41. Moeller BJ, Cao Y, Vujaskovic Z, Li CY, Haroon ZA, Dewhirst MW. The relationship between hypoxia and angiogenesis. Semin Radiat Oncol 2004;14:215–21.
42. Sipos B, Weber D, Ungefroren H, et al. Vascular endothelial growth factor mediated angiogenic potential of pancreatic ductal carcinomas enhanced by hypoxia: an *in vitro* and *in vivo* study. Int J Cancer 2002;102:592–600.
43. Levine L, Lucci JA III, Pazdrak B, et al. Bombesin stimulates nuclear factor kappa B activation and expression of proangiogenic factors in prostate cancer cells. Cancer Res 2003;63:3495–502.
44. Madarame J, Higashiyama S, Kiyota H, et al. Transactivation of epidermal growth factor receptor after heparin-binding epidermal growth factor-like growth factor shedding in the migration of prostate cancer cells promoted by bombesin. Prostate 2003; 57:187–95.

Gastrin Enhances the Angiogenic Potential of Endothelial Cells via Modulation of Heparin-Binding Epidermal-Like Growth Factor

Philip A. Clarke, Jacqueline H. Dickson, Joseph C. Harris, et al.

Cancer Res 2006;66:3504-3512.